# Round Robin Analysis for Probabilistic Structural Integrity of Reactor Pressure Vessel under Pressurized Thermal Shock

**Myung Jo Jhung***, **Changheui Jang, Seok Hun Kim**
**Young Hwan Choi, Hho Jung Kim**
*Korea Institute of Nuclear Safety*
*19 Guseong-dong, Yuseong-gu, Daejeon 305-338, Korea*
**Sunggyu Jung, Jong Min Kim, Gap Heon Sohn, Tae Eun Jin, Taek Sang Choi**
*Korea Power Engineering Company*

**Ji Ho Kim, Jong Wook Kim, Keun Bae Park**
*Korea Atomic Energy Research Institute*

Performed here is a comparative assessment study for the probabilistic fracture mechanics approach of the pressurized thermal shock of the reactor pressure vessel A round robin consisting of one prerequisite deterministic study and five cases for probabilistic approaches is proposed, and all organizations interested are invited The problems are solved by the participants and their results are compared to issue some recommendation of best practices and to assure an understanding of the key parameters in this type of approach, like transient description and frequency, material properties, defect type and distribution, fracture mechanics methodology etc , which will be useful in the justification through a probabilistic approach for the case of a plant over-passing the screening criteria Six participants from 3 organizations responded to the problem and their results are compiled and analyzed in this study

**Key Words :** Probabilistic Analysis, Pressurized Thermal Shock, Reactor Pressure Vessel, Stress Intensity Factor, Fracture Toughness, Residual Stress, Monte Carlo Simulation

## 1. Introduction

A reactor pressure vessel is a critical component of nuclear power plant It contains fuel assemblies and reactor vessel internals and provides flow paths for the coolant of high temperature and high pressure during normal operation. It is designed and manufactured according to strict requirements and regulations Therefore, the structural integrity of the reactor vessel is the most active research subject (Jhung and Park, 1999, Jhung et al, 2003)

Since the Rancho Seco transient in 1978, a pressurized thermal shock (PTS) has been designated as a severe safety issue A pressurized thermal shock involves a transient in which severe overcooling causes a thermal shock to the vessel, while the pressure is either maintained high or the system is repressurized during the transient The thermal stress due to the rapid cooling of the vessel walls in combination with the pressure stress results in large tensile stresses which are maximum at the inside surface of the vessel At temperature below nil ductility temperature of the vessel material, the combination of the pressure and thermal stresses could cause crack propagation through the vessel wall because of the de-

* Corresponding Author,
**E-mail** mjj@kins re kr
**TEL** +82-42-868-0467, **FAX** +82-42-868-0457
Korea Institute of Nuclear Safety, 19 Guseong-dong, Yuseong-gu, Daejeon 305-338 Korea (Manuscript **Received** August 19, 2004, **Revised** November 25, 2004)

crease in fracture toughness. Therefore, it is necessary to evaluate a structural integrity of a reactor pressure vessel (RPV) under a pressurized thermal shock event.

To verify the structural integrity of the reactor vessel against the PTS transients, industries, research centers and regulatory bodies introduce their own methodologies, which need to be verified. In this case, a comparative assessment study is a powerful tool to evaluate the validity of the proposed approaches. Therefore a round robin PROSIR (Probabilistic Structural Integrity of RPV) is proposed by OECD/NEA PWG-3 IAGE Metal Group (Faidy, 2003) as a complementary step to FALSIRE (Bass et al., 1996) and ICAS (Sievers and Schulz, 1999) program on the RPV integrity, and all parties concerned are requested to participate in. It brings together a group of experts from research, utility and regulatory organization to perform a comparative evaluation of analysis methodologies employed in the assessment of RPV integrity under PTS loading conditions. Within the comparative study, analyses of temperature and stress distributions in the vessel wall are performed according to the given material properties and the postulated crack and transients. For the crack, a fracture mechanics assessment is performed to determine the probability of crack initiation (PCI). Random parameters considered are initial $RT_{NDT}$, copper, phosphorus and nickel contents, $RT_{NDT}$ shift, fluence etc.

This paper compiles the results provided by participants in Korea, generating some general results for the probabilistic fracture mechanics analysis of the PTS. Emphasis in the study is placed on the comparison of different approaches to RPV probabilistic integrity assessment employed by the nuclear technology community.

## 2. Problem Definition

### 2.1 Reactor vessel

The reactor vessel considered in the analysis is typical 3-loop PWR with an inner surface radius of 1994 mm, a base metal thickness of 200 mm and a cladding thickness of 7.5 mm. The contents of copper, nickel and phosphorus which augment radiation embrittlement are shown in Table 1 with their corresponding uncertainties. Also irradiation shift formula is defined as Eqs. (1) and (2) for the base metal and welds, respectively (Faidy, 2003).

$$\Delta RT_{NDT}=[17.3+1537\times(P-0.008)+238\times(Cu-0.08)+191\times Ni^2Cu]\times\varphi^{0.35} \quad (1)$$

$$\Delta RT_{NDT}=[18+823\times(P-0.008)-148\times(Cu-0.08)+157\times Ni^2Cu]\times\varphi^{0.45} \quad (2)$$

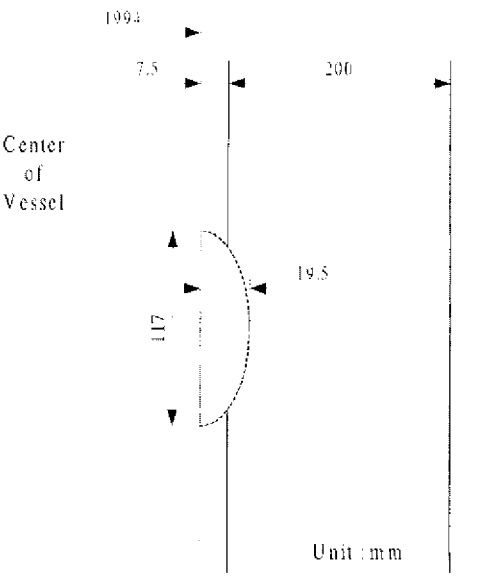


**Fig. 1** Postulated crack

**Table 1** Chemical composition and initial $RT_{NDT}$

| | Initial $RT_{NDT}$ (℃) | | % Copper | | % Phosphorus | | % Nickel | |
|---|---|---|---|---|---|---|---|---|
| | Mean | 1SD* | Mean | 2SD | Mean | 2SD | Mean | 2SD |
| Base metal | −20 | 9 | 0.086 | 0.02 | 0.0137 | 0.002 | 0.72 | 0.1 |
| Welds | −30 | 16 | 0.120 | 0.02 | 0.0180 | 0.002 | 0.17 | 0.1 |

* standard deviation

where $P$, $Cu$ and $Ni$ are weight percent of phosphorus, copper and nickel and $\varphi$ is the fluence in n/m$^2$ divided by $10^{23}$. The uncertainties of $\Delta RT_{NDT}$ are assumed to be 10℃ and 6℃ for base metal and welds, respectively.

The crack postulated is surface breaking crack of 19.5 mm depth ×117 mm length for semi-elliptical through clad crack as shown in Fig. 1. The orientation is longitudinal or circumferential with the base case of longitudinal direction.

### 2.2 Transients

Two overcooling transients due to assumed leaks are defined as in Fig. 2, for which axisymmetric loading conditions are assumed. One is a transient derived from either of the sequences from small loss of coolant accident (SBLOCA) at full power. As shown in Fig. 2, the temperature starts to decrease with cold emergency cooling water injection. System pressure decreases rapidly because the coolant flow rate through the break was greater than the charging and emergency cooling water flow rate. The final coolant temperature is about 7℃. The other transient is typical PTS with re-pressurization. The temperature and pressure start to decrease but at a certain time, about 7200 seconds after the transient began, the system pressure increases rapidly and it is maintained and slow heating occurs, which shows typical characteristics of the PTS transient. In this case pressure is assumed to be a dominant factor.

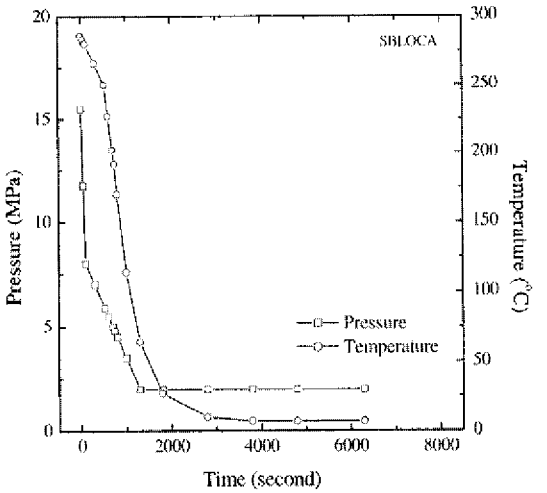


(a) SBLOCA

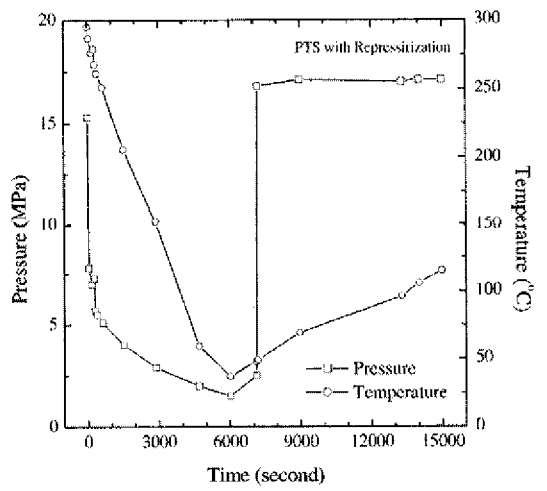


(b) PTS

**Fig. 2** Transient histories for SBLOCA and PTS

### 2.3 Prerequisite study

A deterministic approach based on the mean values of each random parameter is proposed as a prerequisite to assure a perfect fitting at this level of all interesting participants. The crack is located in a longitudinal weld. The crack initiation of surface crack is investigated by direct comparison of $K_I$ and $K_{IC}$. Outputs are required to be prepared such as crack initiation time in the transient, crack tip temperature, toughness at this time and $K_I$ versus time etc. This kind of study is assumed to be a good approach to eliminate the possibility of error which may be encountered in the probabilistic approach by discussing the deterministic results with the different partners before moving to the major round robin.

### 2.4 Major round robins

#### 2.4.1 RR1

This round robin covers toughness property distribution versus aging. The random parameters are initial $RT_{NDT}$, copper, phosphorus and nickel contents and $RT_{NDT}$ shift. The results required are $RT_{NDT}$ distributions of mean value and standard deviation for different levels of fluence (RR1-a). Also, fluence may be included in the random parameters above for different levels

of RPV age (RR1-b).

#### 2.4.2 RR2

The PCI versus time for PTS transient is investigated in this round robin using toughness distribution from RR1. The non-random parameters are vessel, geometry, defect, transient, fluence decrease and material properties. For the fracture mechanics analysis, elastic computation with no plasticity correction is recommended with the assumption that crack initiation occurs only at the deepest point. The results required are the PCI for one defect in welds or in base metal versus vessel age and the time in the transient of the maximum PCI.

#### 2.4.3 RR3

SBLOCA is investigated in this round robin using the same random and non-random parameters of RR2.

#### 2.4.4 RR4

The PCI versus time for one crack in a crack size distribution is investigated in this round robin using the random parameters of RR2 and defect aspect ratio of $a/2l=1/6$. The flaw size distribution of PNNL as shown in Fig. 3 is used as a base case. The non-random parameters and fracture mechanics methodology are the same as RR2. The results required are PCI for one defect in welds or in base metal versus vessel age for PTS transient and time in the transient of the maximum PCI.

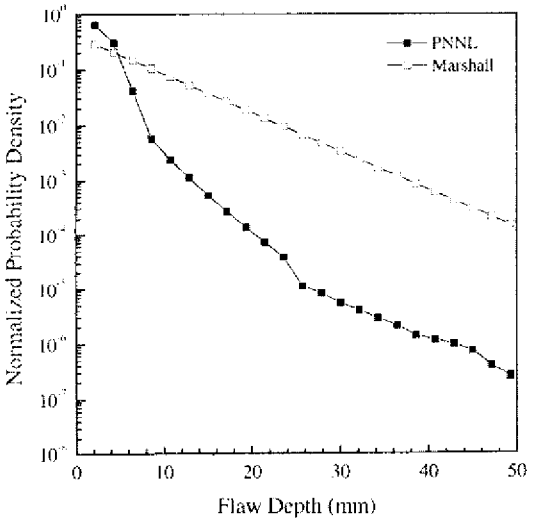


**Fig. 3** Conditional distributions of flaw depth dimensions

#### 2.5 Sensitivity study

Several parametric studies are proposed to investigate the influence of certain parameters on the results of the main tasks. Considered are crack location, flaw distribution, base metal/welds, $RT_{NDT}$ shift formula, residual stress, master curve or other random variables. This study is performed on a volunteer basis.

## 3. Analysis

#### 3.1 Analysis method

The schematic diagram of the probabilistic fracture mechanics analysis is shown in Fig. 4. As shown in Fig. 4, the analysis consists of two

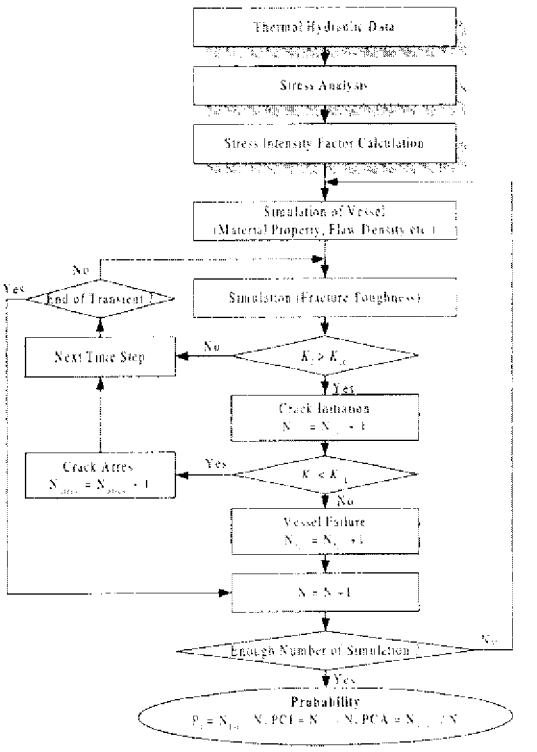


**Fig. 4** Schematic diagram of the probabilistic fracture mechanics analysis

parts, such as the deterministic and probabilistic fracture mechanics analysis In the deterministic analysis part, the temperature profiles along the thickness of the reactor pressure vessel are calculated for the given thermal-hydraulic boundary conditions The distribution of stresses from various sources like thermal, pressure, and residual stresses are separately calculated The resulting stress intensity factors from those stress components are calculated and added to give the applied stress intensity factors $K_I$ at the tip of the flaws In the probabilistic analysis part, variety of statistical parameters such as flaw size, neutron fluence, copper and nickel contents, and $RT_{NDT}$ are simulated for each hypothetical reactor pressure vessel From temperature profile and $RT_{NDT}$, the mean $K_{IC}$ and $K_{IA}$ at the tip of the flaws are calculated using the equation derived from the lower-bound fracture toughness

Finally, fracture toughness values are simulated to be compared with the applied stress intensity factors at the tip of the flaws If $K_I$ is larger than $K_{IC}$, flaw is assumed to initiate and grow a certain distance Then, at the new flaw size, new values of $RT_{NDT}$, $K_I$ and $K_{IA}$ are simulated and compared If $K_I$ is smaller than $K_{IA}$, flaw is considered to be arrested Otherwise, flaw is increased again and the arrest check is repeated

By repeating the above analysis millions of times, statistically significant conditional probability of the vessel failure for a specific thermal hydraulic boundary condition is determined as the number of vessels failed divided by the total number of vessels simulated

### 3.2 $RT_{NDT}$ calculation

The reference temperature of nil-ductility transition $RT_{NDT}$ is given by the following expression,

$$RT_{NDT}=RT_{NDT0}+\Delta RT_{NDT}+M \qquad (3)$$

where $RT_{NDT0}$ is the mean value for the initial (unirradiated) value of $RT_{NDT}$ for the RPV region in which the flaw resides, and $\Delta RT_{NDT}$ is the increase in $RT_{NDT}$ due to irradiation-induced embrittlement, which is a function of the copper and nickel content and neutron fluences corresponding to the RPV region in which the flaw resides The neutron fluence is attenuated to the crack tip and is calculated in accordance with Regulatory Guide 1 99, Revision 2 (USNRC, 1988) $M$ is the margin which considers the uncertainties of $RT_{NDT0}$ and $\Delta RT_{NDT}$, and is calculated as,

$$M=ERRTN\sqrt{(SD_{RT_{NDT0}})^2+(SD_{\Delta RT_{NDT}})^2} \qquad (4)$$

where $SD_{RT_{NDT0}}$ and $SD_{\Delta RT_{NDT}}$ are 1 standard deviation uncertainty for mean value of $RT_{NDT0}$ and $\Delta RT_{NDT}$, respectively. $ERRTN$ is sampled from a Gaussian distribution that has a mean value of 0, a standard deviation of 1, and is truncated at $\pm 3$ standard deviations Therefore, $ERRTN$ varies between $-3$ and $+3$ and is simulated once per vessel $\sqrt{(SD_{RT_{NDT0}})^2+(SD_{\Delta RT_{NDT}})^2}$ is the 1 standard deviation uncertainty. Multiplying it by $ERRTN$ increases the uncertainty to 3 standard deviation $SD_{RT_{NDT0}}$ and $SD_{\Delta RT_{NDT}}$ are combined as the square root of the sum of the squares since they are assumed to be independent

### 3.3 Participants

Six participants from 3 organizations presented the results Participants represent all parties interested in the PTS analysis such as the industry party, research institute and regulatory body in Korea (Table 2) Participants that provided analysis results are identified only by a numeric code in the tables and comparative plots This identification approach preserves anonymity of the contributing participants regarding analysis results The computer codes and approaches employed by the participants are summarized in Table 3, which are subdivided into structural analysis, model used and probabilistic analysis categories Most of participants employed finite element method using commercial codes for the structural analyses as shown in Table 3 The other participants used their own PTS-purpose computer codes employing analytical method For the probabilistic analysis all participants used

**Table 2** Organizations participating in the round robin analysis

| Organization | E-mail |
|---|---|
| Korea Institute of Nuclear Safety | chjang@kins re kr, altong@kins re kr |
| Korea Atomic Energy Research Institute | jhkim12@kaeri re kr, kjwook@kaeri.re.kr |
| Korea Power Engineering Company | csg@kopec co kr, jmkim5@kopec co kr |

**Table 3** Computer codes and approaches in the round robin analysis

| Participant | Structural Analysis | | | Model | Probabilistic Analysis |
|---|---|---|---|---|---|
| | Heat transfer | Stress | Fracture Mechanics | | |
| 1 | PREVIAS | PREVIAS | PREVIAS* | 1-D | PREVIAS |
| 2 | ABAQUS | ABAQUS | Influence Function Method | 2-D | Fortran |
| 3 | ABAQUS | ABAQUS | Influence Function Method | 3-D | PFAP 1 0 |
| 4 | ABAQUS | ABAQUS | ABAQUS | 3-D | Excel |
| 5 | PROBie-Rx | PROBie-Rx | PROBie-Rx** | 1-D | PROBie-Rx |
| 6 | FAVOR 2 4 | FAVOR 2 4 | FAVOR 2 4*** | 1-D | Origin |

* (Jung et al , 2003) ** (Jang et al , 2004) *** (Dickson and Williams, 2003)

their own method, which is incorporated in their own computer code using Fortran program or commercial database program such as Excel

## 4. Results and Discussion

To perform probabilistic fracture analysis for a crack in a reactor vessel wall, the time history of stress distribution in the vessel wall due to the temperature and pressure transient should be estimated If the stress analysis at each time step is carried out in the Monte Carlo simulation process, the time consumption would be excessive To avoid this, the stress analysis should be carried out before Monte Carlo simulation and the stress distribution along the vessel wall at each time step should be approximated to a 3rd order polynomial equation, as follows (ASME, 1998),

$$\sigma=A_0+A_1(x/a)+A_2(x/a)^2+A_3(x/a)^3$$

where $x$ is the distance through the wall thickness direction measured from the inner surface ($0<x/a<1$), and $A_0$, $A_1$, $A_2$, $A_3$ are constants

The stress intensity factor for a surface flaw is then calculated by applying following equation ;

$$K_I=[(A_0+A_p)G_0+A_1G_1+A_2G_2+A_3G_3]\sqrt{\frac{\pi a}{Q}} \quad (6)$$

where $A_p$ is the internal vessel pressure, $G_0$, $G_1$, $G_2$, $G_3$ are free surface correction factors, and $Q$ is the flaw shape parameter using the following equation ,

$$Q=1+4\,593\left(\frac{a}{l}\right)^{1\,65}-q_y \quad (7)$$

where $l$ is the major axis of the flaw, $a/l$ is the flaw aspect ratio and $q_y$ is the plastic zone correction factor calculated using the following equation

$$q_y=\frac{1}{6}[(A_0G_0+A_1G_1+A_2G_2+A_3G_3)/\sigma_{ys}]^2 \quad (8)$$

where $\sigma_{ys}$ is the material yield strength

But, the stress intensity factor obtained by this method varies according to how the stress profile in the vessel wall is approximated because of the stress difference between clad region and base metal region as shown in Fig 5 If the stress in the clad is much higher than that in the base metal, the approximated stress obtained by 3rd polynomial curve fitting with all nodal stresses is overestimated (Approx-1) On the contrary, if the cladding stress is ignored the approximated stress is underestimated (Approx-3) Approx-2 of Fig 5 is the case that the mean stress at the boundary of the clad and base metal is considered as the only clad stress The resulting stress

intensity factors for the different approximation methods are shown in Fig. 6, which shows that stress approximation should be carefully carried out considering the stress profile in both the clad and base metal.

Meanwhile, one of the participants used different approach to calculate the stress intensity factor (Jang et al., 2003). He calculated the stresses from various sources, such as thermal, pressure and residual stresses. He further divided the thermal stress components into clad stress confined within the narrow cladding and base stress. The stress intensity factor components calculated for the stress components are added to be the stress intensity factor at the crack tip. In this approach, the uncertainty associated the stress approximation is avoided.

Temperature and stress intensity factor histories at crack tip from participants are compared in Figs. 7 and 8, respectively. The temperature is almost the same at crack tip but the stress intensity factors have some differences among participants. Even though the stresses are the same, the methods to calculate the stress intensity factor are

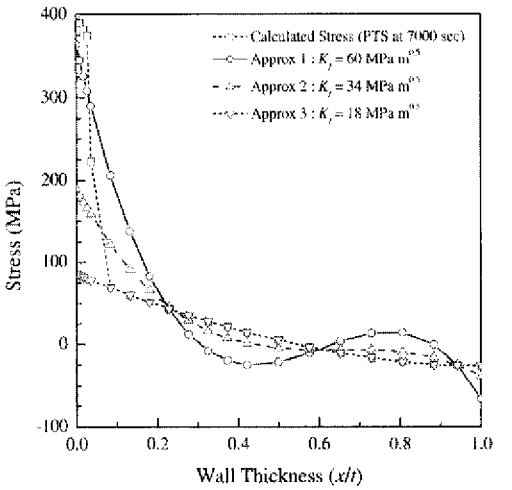


**Fig. 5** $K_I$ variations according to stress approximation

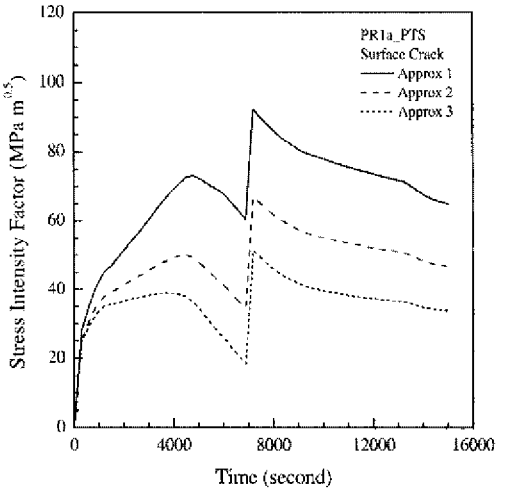


**Fig. 6** Comparison of $K_I$ according to stress approximation

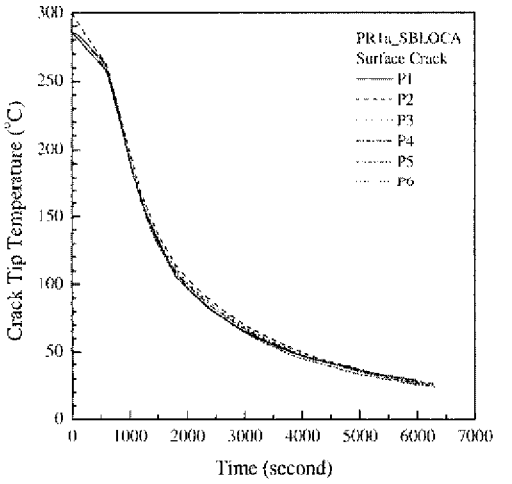


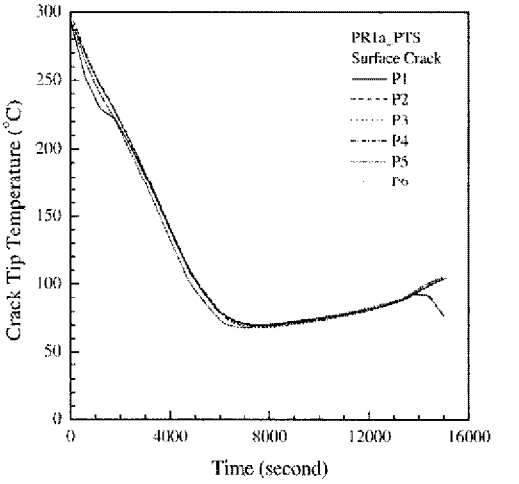


**Fig. 7** Comparison of crack tip temperature

different as shown in Table 3, generating some differences among participants. Also, deterministic approaches among participants are a little bit different as shown in Table 4. This may be a major factor to affect the results of the probabilistic approaches.

The comparison of methods to calculate the adjusted $RT_{NDT}$ is shown in Table 5. All participants except participant 6 used the formula of Eq. (3). In this case the mean value of $RT_{NDT0}$ and mean formula of $RT_{NDT}$ are used. Participant 6 simulated $RT_{NDT0}$ and $RT_{NDT}$. In this case the uncertainties of $RT_{NDT0}$ and $RT_{NDT}$ are already included and therefore it is not necessary to include margin term $M$ to calculate $RT_{NDT}$. These two approaches should give the same results as shown in Fig. 9. Participant 1 simulated $RT_{NDT0}$ and the value of $\sqrt{(SD_{RT_{NDT}})^2+(SD_{\Delta RT_{NDT}})^2}$ in the margin term and at the same time used depth as a random variable for $\Delta RT_{NDT}$, which caused big difference in the adjusted $RT_{NDT}$ calculation. The high $RT_{NDT}$ of participant 1 generates low value of $K_{IC}$ and therefore high value of the PCI.

The maximum calculated conditional probabilities of crack initiation as shown in Fig. 10, especially for small values of fluence, have the largest scatter, i.e. about a factor of 100 when not considering the result of participant 1, which is

**Table 4** Comparison of method for deterministic approach

| Participant | Stress free temperature (℃) | Material property variation with temperature | $K$ estimation scheme | Cladding |
|---|---|---|---|---|
| 1 | 300 | No | Influence coefficient from VISA | Considered |
| 2 | 300 | Yes | Influence coefficient from PROSIR | Considered |
| 3 | 286 | Yes | Influence coefficient from PROSIR | Considered |
| 4 | 286 | Yes | Directly from the finite element analysis | Considered |
| 5 | 300 | No | Influence coefficient independently developed | Considered |
| 6 | 300 | No | Influence coefficient from FAVOR | Considered |

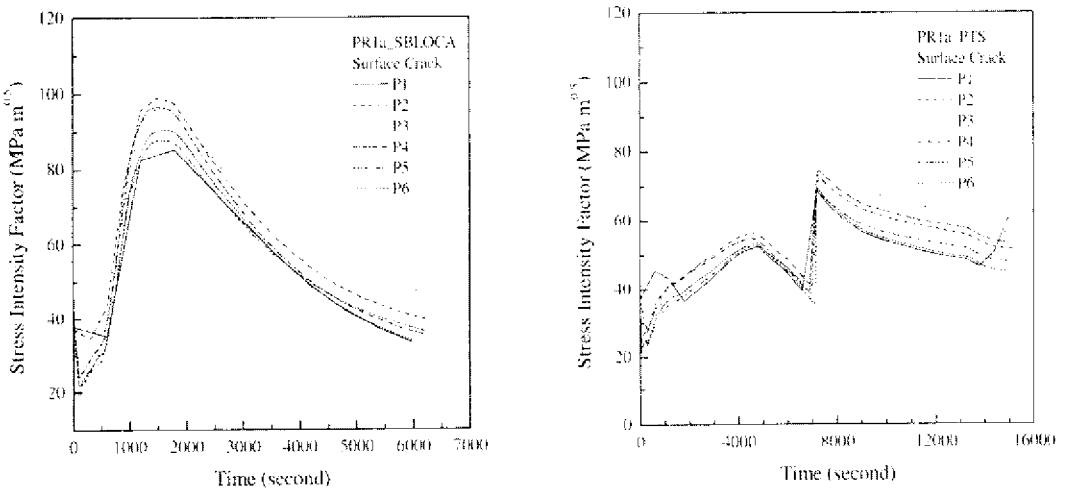


**Fig. 8** Comparison of stress intensity factors at crack tip

**Table 5** Comparison of method to calculate $RT_{NDT}$

| Participant | $RT_{NDT0}$ | Chemistry Factor ($Cu$, $Ni$, $P$) | $\Delta RT_{NDT}$ | $SD_{RT_{NDT0}}$ $SD_{\Delta RT_{NDT}}$ | Margin, $M$ | $RT_{NDT}$ |
|---|---|---|---|---|---|---|
| 1 | Simulation | Simulation | Mean | Fixed value | Simulation of $\sqrt{(SD_{RT_{NDT0}})^2+(SD_{\Delta RT_{NDT}})^2}$ | $RT_{NDT0}+\Delta RT_{NDT}+M$ |
| 2 | Mean | Simulation | Mean | Fixed value | Simulated value $\times$ $\sqrt{(SD_{RT_{NDT0}})^2+(SD_{\Delta RT_{NDT}})^2}$ | $RT_{NDT0}+\Delta RT_{NDT}+M$ |
| 3 | Mean | Simulation | Mean | Fixed value | Simulated value $\times$ $\sqrt{(SD_{RT_{NDT0}})^2+(SD_{\Delta RT_{NDT}})^2}$ | $RT_{NDT0}+\Delta RT_{NDT}+M$ |
| 4 | Mean | Simulation | Mean | Fixed value | Simulated value $\times$ $\sqrt{(SD_{RT_{NDT0}})^2+(SD_{\Delta RT_{NDT}})^2}$ | $RT_{NDT0}+\Delta RT_{NDT}+M$ |
| 5 | Mean | Simulation | Mean | Fixed value | Simulated value $\times$ $\sqrt{(SD_{RT_{NDT0}})^2+(SD_{\Delta RT_{NDT}})^2}$ | $RT_{NDT0}+\Delta RT_{NDT}+M$ |
| 6 | Simulation | Simulation | Simulation | | | $RT_{NDT0}+\Delta RT_{NDT}$ |

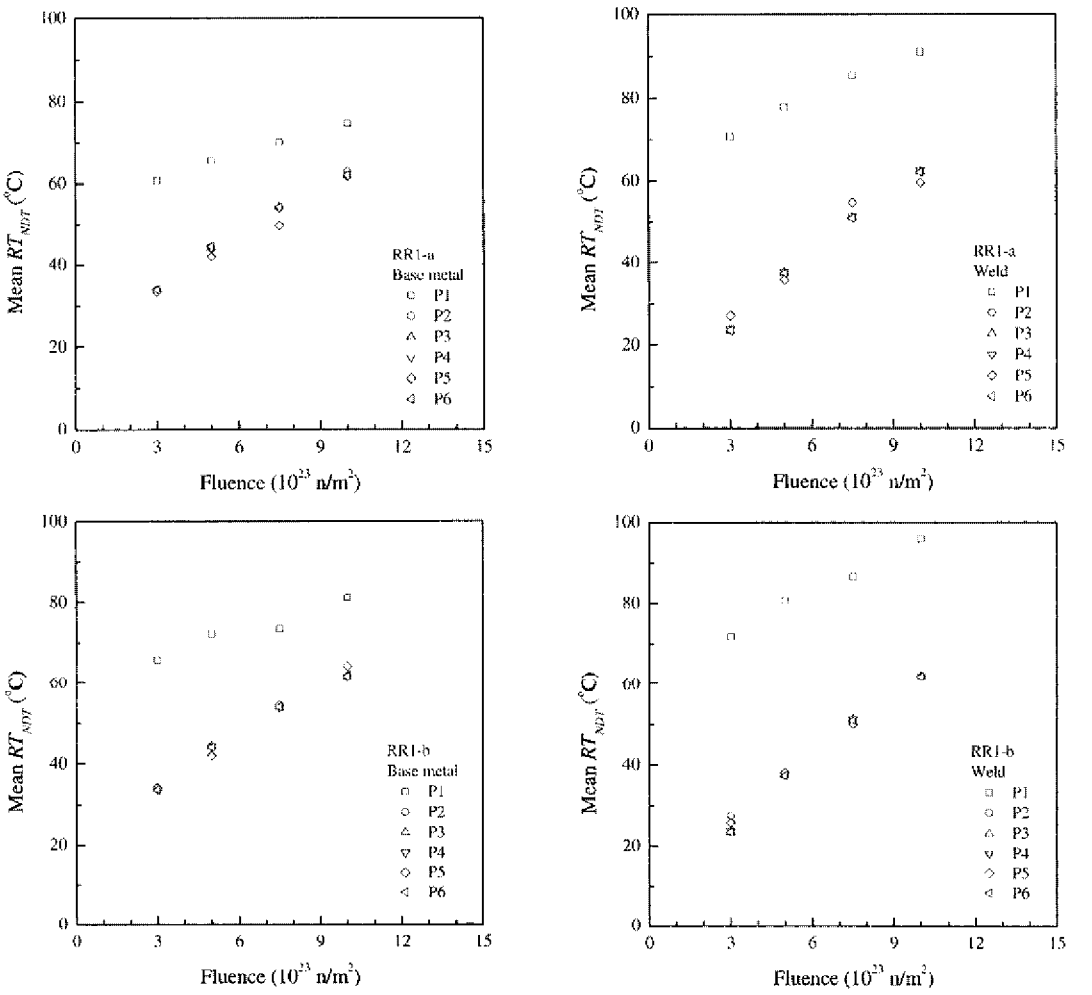


**Fig. 9** Mean $RT_{NDT}$

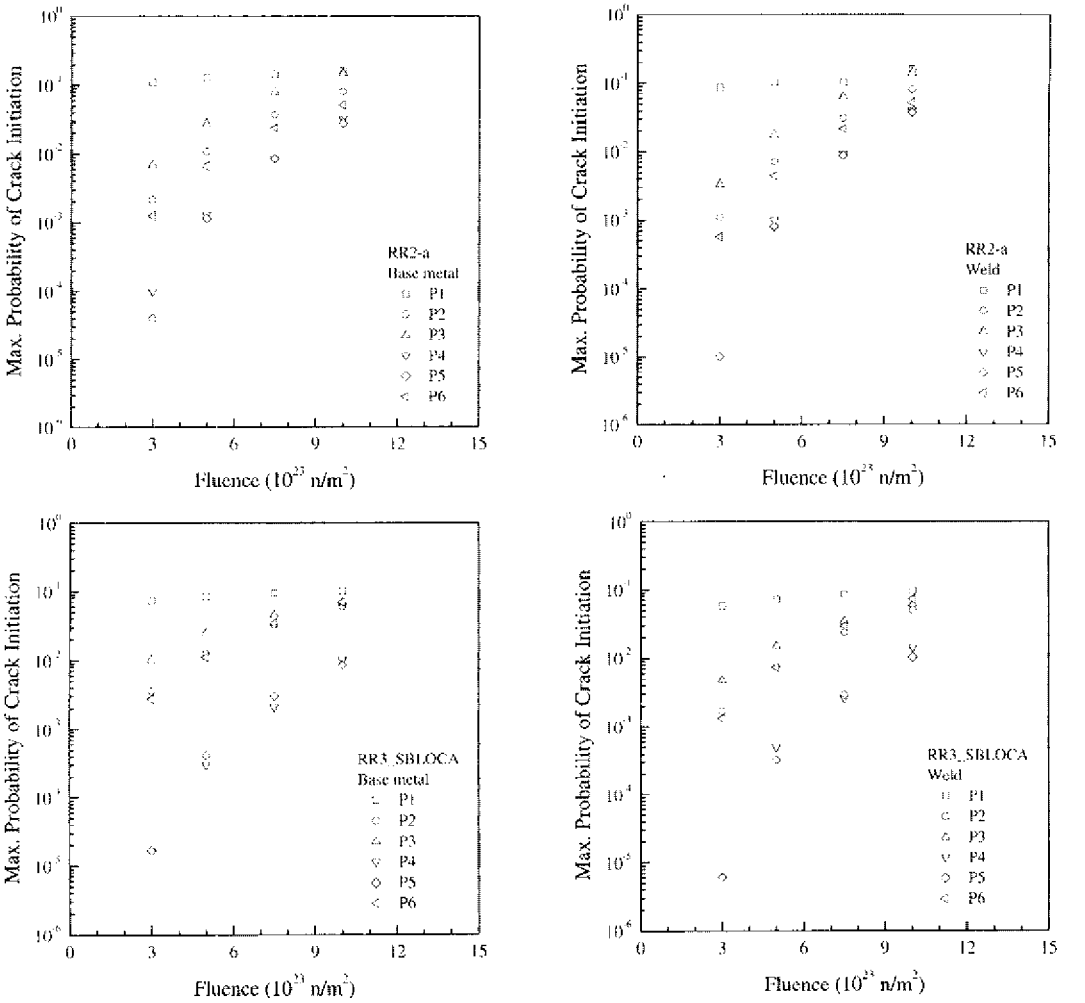


**Fig. 10** Maximum probability of crack initiation

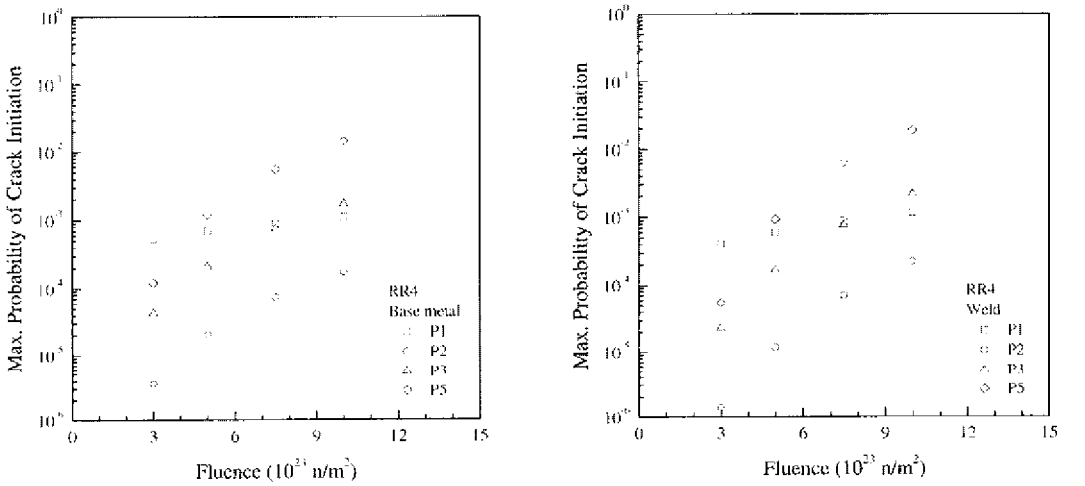


**Fig. 11** Maximum probability of crack initiation considering defect aspect ratio

presumably due to the over-estimation of $RT_{NDT}$ by using different schemes of for the $RT_{NDT}$ simulation. The results of participants 4 and 5 are relatively lower than those of others and show strong dependency on the fluence level. The maximum PCI considering defect aspect ratio is shown in Fig. 11. It has similar trend described above but is so small compared to that of Fig. 10 and therefore it is evident that including random variable of defect aspect ratio decreases the PCI significantly, more than 2 orders of magnitude in this case.

The PCI versus time is shown in Fig. 12 for fluence of $3\times10^{23}$ n/m$^2$. The time in the transient of the maximum PCI for SBLOCA comes earlier than that for PTS, which can be predicted from Fig. 2 where maximum PCI occurs at the instant of rapid decrease of pressure and temperature. But for PTS transient the instant of repressurization is more important than that of rapid decrease of temperature and/or pressure.

Several sensitivity analyses investigating the

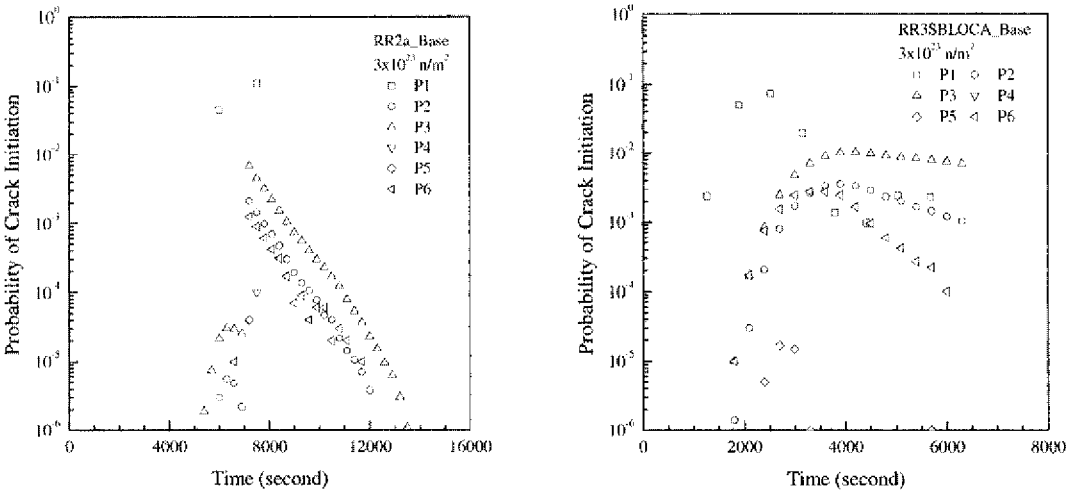


(a) PTS (b) SBLOCA

**Fig. 12** Probability of crack initiation versus time

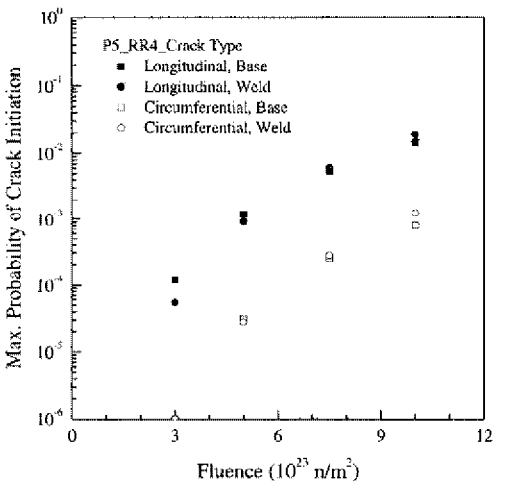


**Fig. 13** Maximum probability of crack initiation according to crack type

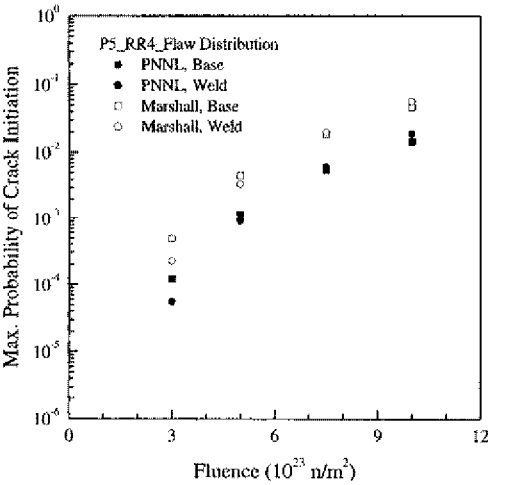


**Fig. 14** Maximum probability of crack initiation according to flaw distribution

effects of parameters such as crack location, flaw distribution, base metal/welds, $RT_{NDT}$ shift, residual stress and master curve are performed. Figure 13 shows the maximum PCI for crack location. Circumferential and longitudinal cracks are assumed and the maximum PCI of circumferential crack is lower than that of longitudinal crack by one to two orders of magnitude. The stresses on circumferential flaw due to pressure are one half of those on longitudinal flaw and therefore lower stress intensity factors are obtained. If the transient is dominated by pressure loading like typical PTS event, less initiation for circumferential crack is expected.

Two types of flaw distribution of Fig. 3 are considered where Marshall assumes larger flaws, which are subjected to high stress intensity factors and therefore higher initiation occurs as shown in Fig. 14.

The comparison of $RT_{NDT}$ shift formula is made in Fig. 15, where $\Delta RT_{NDT}$ of Regulatory Guide 1.99 is considerably small compared with that of Eqs. (1) and (2). Also the maximum PCI of Regulatory Guide 1.99 is considerably small as shown in Fig. 16 by two orders of magnitude compared with that of PROSIR where Eqs. (1) and (2) are used. This may indicate that $RT_{NDT}$ shift formula of Regulatory Guide 1.99 may not be conservative in a certain circumstance.

The maximum probabilities of crack initiation are obtained for different toughness curves of Fig. 17 where mean values of $K_{IC}$ and $K_{IA}$ from PROSIR and master curve (USNRC, 1998) are compared. When the same values of $RT_{NDT}$ are used, the maximum PCI for master curve is larger than that of PROSIR by one to two orders of magnitude and the difference gets more significant for the lower level of fluence as shown in Fig. 18. This is due to the fact that mean minus 3 standard deviation values of fracture toughness for master curve are lower than those of PROSIR even

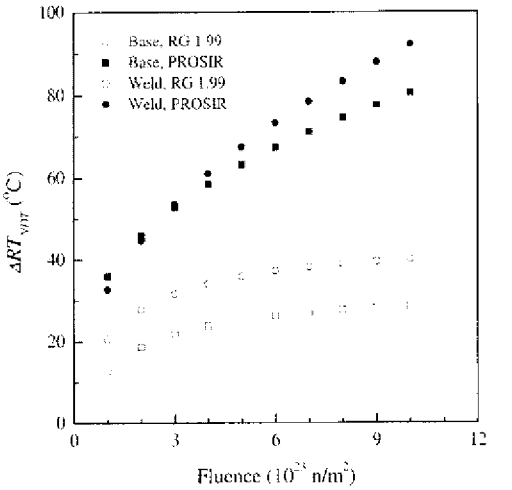


**Fig. 15** Comparison of $RT_{NDT}$ shift

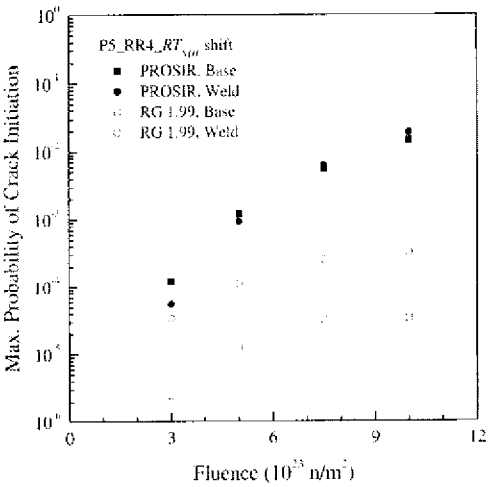


**Fig. 16** Maximum probability of crack initiation according to $RT_{NDT}$ shift

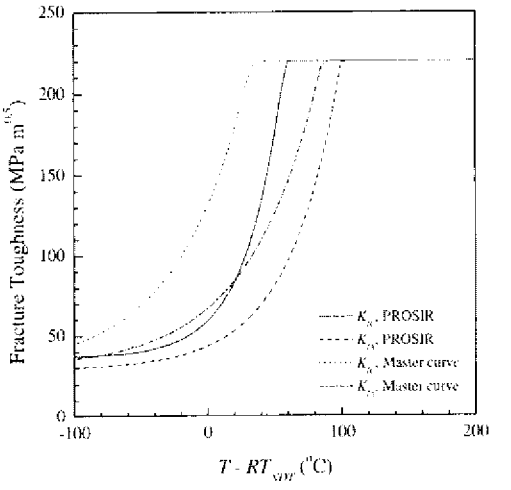


**Fig. 17** Comparison of mean fracture toughness curves

though mean curves are opposite for the same $RT_{NDT}$ (Fig. 19). Also it is noted that the level of fluence do not affect the PCI significantly for the case of master curve.

The effect of residual stress on the PCI is investigated. The residual stress of Fig. 20 is assumed and the maximum probabilities of crack initiation are obtained as shown in Fig. 21. Residual stress increases the stress intensity factor and crack initiation. The maximum PCI increased by the factor of about 2 by including the residual stress. The effect of residual stress could have been greater for the less significant PTS transient, but for the relatively severe transient like typical PTS event with pressure dominant, the effect on the PCI is not so significant because most of the weak links are already broken.

The maximum probabilities of crack initiation of welds are larger than those of base metal for Regulatory Guide 1.99 by about one order of magnitude but they are almost the same for PROSIR. This kind of difference between base metal and welds is shown for all maximum pro-

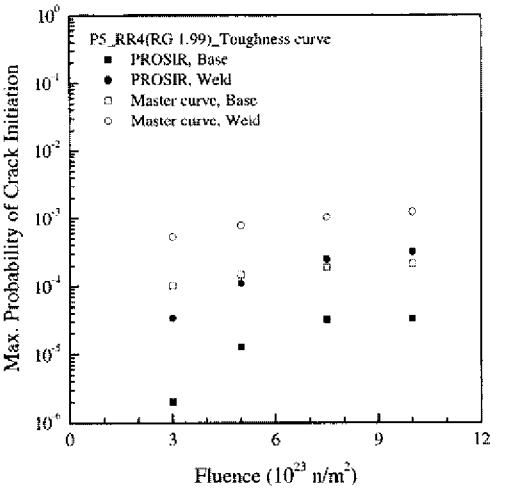


**Fig. 18** Maximum probability of crack initiation according to toughness curve

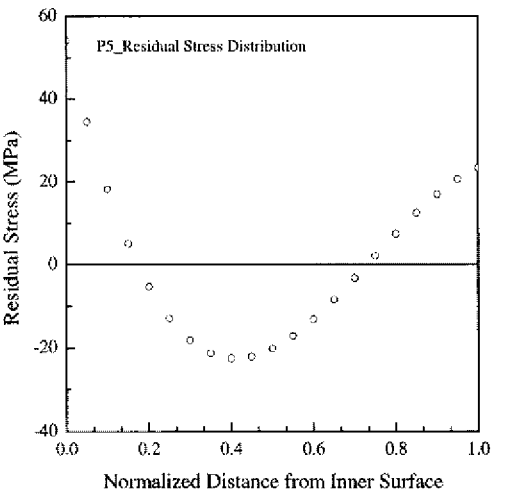


**Fig. 20** Residual stress distribution

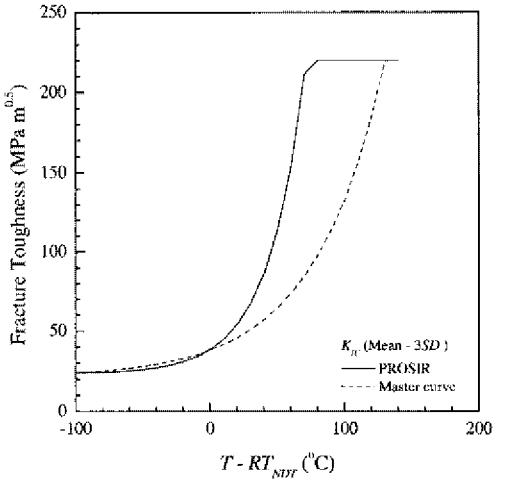


**Fig. 19** Comparison of mean$-3SD$ for fracture toughness curves

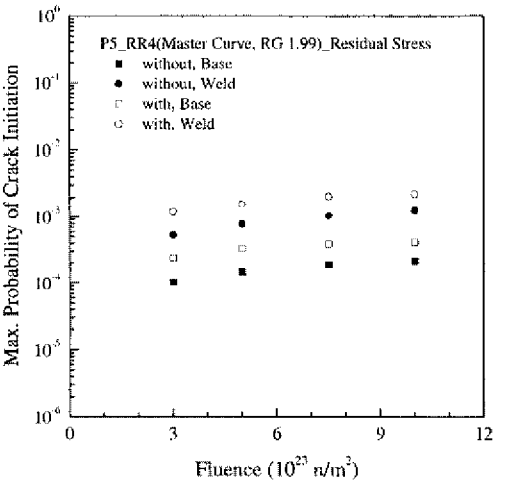


**Fig. 21** Maximum probability of crack initiation according to residual stress

babilities of crack initiation of Figs 18 and 21 where $RT_{NDT}$ shift formula from Regulatory Guide 1 99 is used irrespective of toughness curve or residual stress.

## 5. Conclusions

Round robin analyses of the reactor pressure vessel under the pressurized thermal shock are performed using the information of OECD/NEA PWG3 Two transients and one crack are postulated and the probabilistic fracture mechanics analyses are performed to generate the conditional probabilities of crack initiation Results from participants are compared generating following conclusions

(1) The calculated probabilities of crack initiation have the scatter differing among participants, which are apparently caused by the difference of stress intensity factors among participants and the selection of different input parameters for $RT_{NDT}$ simulation

(2) Special care should be taken to calculate the stress intensity factor by approximating the stress distribution of the cladding region by polynomial expression

(3) The maximum PCI may be lowered by the factor of 100 according to the crack location, flaw distribution and $RT_{NDT}$ shift formula

(4) The effect of increasing fluence on the PCI is small when using the master curve method Therefore for the life extension it would be a good try to adopt a master curve for the fracture toughness

(5) The maximum PCI of welds is always larger than that of base metal by the factor of about 10 when $RT_{NDT}$ shift formula from Regulatory Guide 1 99 is used

## References

ASME, 1998, ASME Boiler and Pressure Vessel Code, Section XI Rules for Inspection of Nuclear Power Plant Components, Appendix A Analysis of Flaws, The American Society of Mechanical Engineers

Bass, B R, Pugh, C E, Keeney, J, Schulz, H and Sievers, J, 1996, "CSNI Project for Fracture Analysis of Large-Scale International Reference Experiments (FALSIRE II)," NEA/CSNI/R(96) 1, OECD/NEA, November

Dickson, T L and Williams, P T, 2003, Fracture Analysis of Vessels - Oak Ridge FAVOR, v02 4, Computer Code Theory and Implementation of Algorithms, Methods and Correlations, draft NUREG, US Nuclear Regulatory Commission

Faidy, C, 2003, PROSIR - Probabilistic Structural Integrity of a PWR Reactor Pressure Vessel, Proposed to OECD/NEA PWG3 - Metal Group, EDF - SEPTEN, July

Jang, C, Kang, S. C, Moonn, H R, Jeong, I S and Kim, T R, 2003, "The Effects of the Stainless Steel Cladding in Pressurized Thermal Shock Evaluation," *Nuclear Engineering and Design*, Vol 226, pp 127~140

Jang, C, Jhung, M J, Kang, S C and Choi, Y H, 2004, "The Effect of Analysis Variables on the Failure Probability of the Reactor Pressure Vessel by Pressurized Thermal Shock," *Transactions of the Korean Society of Mechanical Engineers (A)*, Vol 28, No 6, pp 693~700.

Jhung, M J, Kim, S H, Lee, J H and Park, Y W, 2003, "Round Robin Analysis of Pressurized Thermal Shock for Reactor Pressure Vessel," *Nuclear Engineering and Design*, Vol 226, pp 141~154

Jhung, M J and Park, Y W, 1999, "Deterministic Structural and Fracture Mechanics Analyses of Reactor Pressure Vessel for Pressurized Thermal Shock," *Structural Engineering and Mechanics*, Vol 8, No 1, pp 103~118

Jung, S G, Jin, T E, Jhung, M J and Choi, Y H, 2003, "Probabilistic Fracture Mechanics Analysis of Reactor Vessel for Pressurized Thermal Shock - The Effect of Residual Stress and Fracture Toughness -," *Transactions of the Korean Society of Mechanical Engineers (A)*, Vol 27, No 6, pp 987~996

Sievers, J and Schulz, H, 1999, "Final Report on the International Comparative Assessment Study of Pressurized - Thermal - Shock in Reactor Pressure Vessels (RPV PTS ICAS)," NEA/

CSNI/R(99)3, OECD/NEA, May

USNRC, 1988, Radiation embrittlement of reactor vessel materials, Regulatory Guide 1.99, Revision 2, U.S Nuclear Regulatory Commission.

USNRC, 1998, Technical Basis for an ASTM Standard on Determining the Reference Temperature, To, for Ferritic Steels in Transition Range, NUREG/CR-5504, US Nuclear Regulatory Commission